

On the Connection Between Gramian-based and Interpolation-based Model Order Reduction

Umair Zulfiqar, Zhi-Hua Xiao, Qiu-yan Song, and Victor Sreeram, *Senior Member, IEEE*

Abstract—Gramian-based model order reduction methods, like balanced truncation, and interpolation-based methods, such as \mathcal{H}_2 -optimal reduction, are two important types of model reduction algorithms. Although both are known for their accuracy, they are often seen as two different approaches. This paper shows that these two methods are closely related, with Gramian-based reduction being roughly an interpolation problem, and vice versa.

For Galerkin projection, we find that when the reduced model has enough order to capture the significant eigenvalues of the controllability or observability Gramian, preserving these eigenvalues becomes an interpolation problem. In this case, both Gramian-based and interpolation-based model reduction methods produce the same transfer function but with different state-space realizations. When the reduced model's order is too small to capture all significant eigenvalues, the methods begin to differ, and the difference depends on the eigenvalues that were left out.

In the case of Petrov-Galerkin projection, if the reduced model's order is large enough to capture the significant Hankel singular values, balanced truncation becomes the same as \mathcal{H}_2 -optimal model order reduction. Again, both methods give the same transfer function but with different state-space realizations. When the order is smaller, the methods diverge, with the difference depending on the truncated Hankel singular values.

Numerical examples are provided to support these findings, showing that Gramian-based and interpolation-based model reduction methods are more connected than previously thought and can be viewed as approximations of each other.

Index Terms—Balanced truncation, Gramians, \mathcal{H}_2 -optimal, Hankel singular values, Hermite interpolation, projection, tangential directions.

I. INTRODUCTION

THE complexity of modern dynamical systems has been growing rapidly, along with the increasing computational power of the computers used for modeling them. However, simulating, analyzing, and designing these high-order systems poses a significant computational challenge due to limited memory resources. Model Order Reduction (MOR) addresses this issue by producing a reduced-order approximation of the original high-order model. This reduced-order model (ROM) serves as a surrogate for the original system, offering a similar level of accuracy with manageable numerical error. ROMs are

more efficient to simulate and analyze, while still retaining the key characteristics of the original system. For further details on this topic, readers are referred to [1]-[5] and the references therein.

Balanced Truncation (BT) [6] is a state-of-the-art classical MOR method, renowned for its accuracy, stability preservation, and well-defined error bounds [7]. BT retains the most controllable and observable states while truncating the less significant ones. It preserves the dominant Hankel singular values, which represent the contribution of each state to the system's overall energy transfer. Over time, BT has been extended into a broader family of techniques known as Gramian-based MOR methods. For a detailed survey of BT and its extensions, see [8]. A key limitation of BT is the computational expense of solving Lyapunov equations to compute the Gramians, especially for high-order systems. To mitigate this, low-rank approximations of the Gramians are used, reducing the computational cost significantly [9].

Interpolation-based MOR, also known as moment matching, represents another key class of MOR algorithms. In these methods, the ROM matches the original system's transfer function at specific points in the s -plane, referred to as interpolation points. These methods are computationally more efficient than BT, as they do not require solving high-order Lyapunov equations. However, the accuracy of the approximation relies heavily on the choice of interpolation points, which is often not straightforward. It has been shown in [10], [11] that the \mathcal{H}_2 -optimal MOR problem, introduced in [12], can be viewed as an interpolation problem with specific interpolation points—namely, the mirror images of the ROM's poles. In the “Iterative Rational Krylov Algorithm (IRKA)” [10], the interpolation points are updated iteratively until convergence. IRKA is one of the state-of-the-art MOR algorithms, recognized for its accuracy, automatic selection of interpolation points, and computational efficiency. A more general approach for solving the \mathcal{H}_2 -optimal MOR problem, based on Sylvester equations, was proposed in [13], with improved computational efficiency in [14]. This method, known as the “Two-sided Iteration Algorithm (TSIA),” is equivalent to IRKA when both the original system and the ROM have simple poles. For a thorough review of interpolation or moment matching methods, see [15]-[17] and the references therein.

BT and \mathcal{H}_2 -optimal MOR algorithms, such as IRKA and TSIA, are generally considered distinct classes of MOR techniques. Recently, efforts have been made to construct the same ROM that BT produces using interpolation methods [18], [19]. These attempts are motivated by the fact that interpolation or moment matching methods are computationally more efficient

U. Zulfiqar is with the School of Electronic Information and Electrical Engineering, Yangtze University, Jingzhou, Hubei, 434023, China (email: uwa.umair@gmail.com)

Z. Xiao is with the School of Information and Mathematics, Yangtze University, Jingzhou, Hubei, 434023, China (email: zhxiao@yangtzeu.edu.cn)

Q. Song is with the School of Mechatronic Engineering and Automation, Shanghai University, Shanghai 200072, China (e-mail: duxin@shu.edu.cn, qysong@shu.edu.cn).

V. Sreeram is with the School of Electrical, Electronics and Computer Engineering, The University of Western Australia, 35 Stirling Highway, Crawley, 6009 Western Australia (email: victor.sreeram@uwa.edu.au).

than BT, as they avoid the need to solve high-order Lyapunov equations. While these initial efforts have not led to significant solutions, they have provided a motivation for further research in this direction. This paper attempts the same problem but notes that IRKA and TSIA already produce nearly the same ROM as BT, as long as the reduced model's order is sufficient to capture all significant Hankel singular values. Therefore, there may be no need to reinvent the wheel.

This paper first presents the key differences between Gramian-based and interpolation-based MOR approaches. It is demonstrated that, while the projection matrices in both methods satisfy Sylvester equations, there are notable differences in these equations. The problem of retaining the most controllable or observable states while truncating the others is then examined, showing that it corresponds to a Galerkin projection problem. This reduces to a subset of the \mathcal{H}_2 -optimal MOR problem when the truncated states are poorly controllable or observable. Additionally, it is shown that the BT problem reduces to an \mathcal{H}_2 -optimal MOR problem when the truncated states are associated with negligible Hankel singular values. Moreover, the \mathcal{H}_2 -optimal MOR problem is approximately a Hankel singular value preservation problem, as the \mathcal{H}_2 norm of the error depends on whether the ROM captures the most controllable and observable states. Two numerical examples are provided to support these findings. The results confirm that BT and IRKA/TSIA can be viewed as approximate versions of each other. BT approximately satisfies the Hermite interpolation conditions and exactly preserves the dominant Hankel singular values, while IRKA/TSIA, upon convergence, exactly satisfies the Hermite interpolation conditions and approximately preserves the Hankel singular values.

II. PRELIMINARIES

Consider an n^{th} -order stable, minimal, linear time-invariant system $H(s)$ with m inputs and p outputs, represented by the state-space realization (A, B, C) as follows:

$$H(s) = C(sI - A)^{-1}B. \quad (1)$$

In this representation, $A \in \mathbb{R}^{n \times n}$ is the state matrix, $B \in \mathbb{R}^{n \times m}$ is the input matrix, and $C \in \mathbb{R}^{p \times n}$ is the output matrix. The state-space equations for the system in (1) are:

$$\begin{aligned} \dot{x}(t) &= Ax(t) + Bu(t), \\ y(t) &= Cx(t). \end{aligned}$$

The controllability Gramian P and observability Gramian Q for the system in (1) are the solutions of the following Lyapunov equations:

$$\begin{aligned} AP + PA^T + BB^T &= 0, \\ A^TQ + QA + C^TC &= 0. \end{aligned}$$

Consider an r^{th} -order reduced model $H_r(s)$ of $H(s)$, with its state-space realization (A_r, B_r, C_r) described by:

$$H_r(s) = C_r(sI - A_r)^{-1}B_r, \quad (2)$$

where $A_r \in \mathbb{R}^{r \times r}$, $B_r \in \mathbb{R}^{r \times m}$, and $C_r \in \mathbb{R}^{p \times r}$. This reduced model $H_r(s)$ is obtained through Petrov-Galerkin projection:

$$A_r = W_r^T A V_r, \quad B_r = W_r^T B, \quad C_r = C V_r,$$

where $V_r \in \mathbb{R}^{n \times r}$ and $W_r \in \mathbb{R}^{n \times r}$, with the condition $W_r^T V_r = I$. The state-space equations for this reduced model are:

$$\begin{aligned} \dot{x}_r(t) &= A_r x_r(t) + B_r u(t), \\ y_r(t) &= C_r x_r. \end{aligned} \quad (3)$$

The controllability Gramian P_r and the observability Gramian Q_r for the reduced model in (2) are the solutions to the following Lyapunov equations:

$$\begin{aligned} A_r P_r + P_r A_r^T + B_r B_r^T &= 0, \\ A_r^T Q_r + Q_r A_r + C_r^T C_r &= 0. \end{aligned}$$

Remark 1: If V_r and W_r are replaced by $V_r R$ and $W_r S$, respectively, where R and S are invertible matrices, they will still produce the same ROM $H_r(s)$, but with a different state-space realization [20].

A. Review of Interpolation-based MOR [15], [17], [20], [21]

Let $S_b \in \mathbb{R}^{r \times r}$, $L_b \in \mathbb{R}^{m \times r}$, $S_c \in \mathbb{R}^{r \times r}$, and $L_c \in \mathbb{R}^{p \times r}$ be matrices such that the pairs (S_b, L_b) and (S_c, L_c) are observable. The projection matrices V_r and W_r are then computed by solving the following Sylvester equations:

$$A V_r - V_r S_b + B L_b = 0, \quad (4)$$

$$A^T W_r - W_r S_c + C^T L_c = 0. \quad (5)$$

Next, we decompose S_b and S_c into their eigenvalue decompositions as follows:

$$S_b = T_{sb}^{-1} \begin{bmatrix} \nu_1 & \cdots & 0 \\ \vdots & \ddots & \vdots \\ 0 & \cdots & \nu_r \end{bmatrix} T_{sb}, \quad S_c = T_{sc}^{-1} \begin{bmatrix} \mu_1 & \cdots & 0 \\ \vdots & \ddots & \vdots \\ 0 & \cdots & \mu_r \end{bmatrix} T_{sc}.$$

Here, ν_i and μ_i are the right and left interpolation points, respectively, and their associated right and left tangential directions are defined as:

$$[b_1 \quad \cdots \quad b_r] = L_b T_{sb}^{-1}, \quad [c_1 \quad \cdots \quad c_r] = L_c T_{sc}^{-1}.$$

The ROM generated by V_r and $W_r S$ (where $S = (V_r^T W_r)^{-1}$) from equations (4) and (5) satisfies the following tangential interpolation conditions:

$$H(\nu_i) b_i = H_r(\nu_i) b_i, \quad \text{and} \quad c_i^T H(\mu_i) = c_i^T H_r(\mu_i).$$

It is important to note, as mentioned in Remark 1, that the matrix S does not alter the ROM $H_r(s)$ produced by the pair (V_r, W_r) , but it ensures the Petrov-Galerkin projection condition $W_r^T V_r = I$ is met. When $\nu_i = \mu_i$, the Hermite interpolation conditions are satisfied as follows:

$$c_i^T H'(\nu_i) b_i = c_i^T H_r'(\nu_i) b_i.$$

B. Review of \mathcal{H}_2 -optimal MOR [10], [11], [13]

Let \hat{P} and \hat{Q} be the solutions to the following Sylvester equations:

$$A \hat{P} + \hat{P} A^T + B B^T = 0, \quad (6)$$

$$A^T \hat{Q} + \hat{Q} A + C^T C = 0. \quad (7)$$

The \mathcal{H}_2 norm of the error between $H(s)$ and $H_r(s)$ is given by:

$$\begin{aligned} \|H(s) - H_r(s)\|_{\mathcal{H}_2} &= \sqrt{CPC^T + 2C\hat{P}C_r^T + C_rP_rC_r^T} \\ &= \sqrt{B^TQB + 2B^T\hat{Q}B_r + B_r^TQ_rB_r}. \end{aligned}$$

The following necessary conditions must be met for a local optimum of $\|H(s) - H_r(s)\|_{\mathcal{H}_2}^2$:

$$C\hat{P} - C_rP_r = 0, \quad (8)$$

$$\hat{Q}^TB - Q_rB_r = 0, \quad (9)$$

$$\hat{Q}^T\hat{P} - Q_rP_r = 0. \quad (10)$$

In [13], TSIA is introduced, which satisfies these optimality conditions (8)–(10) at convergence. Starting with an initial guess for the ROM (A_r, B_r, C_r) , TSIA iteratively updates the projection matrices as $V_r = \hat{P}$ and $W_r = \hat{Q}S$, where $S = (\hat{P}^T\hat{Q})^{-1}$, until convergence is achieved.

Assume that both $H(s)$ and $H_r(s)$ have simple poles. In this case, they can be expressed in the following pole-residue form:

$$H(s) = \sum_{j=1}^n \frac{l_j r_j^*}{s - \lambda_j}, \quad H_r(s) = \sum_{j=1}^r \frac{\tilde{l}_j \tilde{r}_j^*}{s - \tilde{\lambda}_j}.$$

The optimality conditions (8)–(10) then simplify to the following Hermite interpolation conditions:

$$H(-\tilde{\lambda}_i)\tilde{r}_i = H_r(-\tilde{\lambda}_i)\tilde{r}_i, \quad (11)$$

$$\tilde{l}_i^* H(-\tilde{\lambda}_i) = \tilde{l}_i^* H_r(-\tilde{\lambda}_i) \quad (12)$$

$$\tilde{l}_i^* H'(-\tilde{\lambda}_i)\tilde{r}_i = \tilde{l}_i^* H_r'(-\tilde{\lambda}_i)\tilde{r}_i. \quad (13)$$

IRKA [10], a pioneering and efficient \mathcal{H}_2 -optimal MOR algorithm, ensures that the interpolation conditions (11)–(13) are satisfied upon convergence. Starting with arbitrary interpolation points and tangential directions, IRKA updates the interpolation data triplet $(\nu_i, b_i, c_i) = (-\tilde{\lambda}_i, \tilde{r}_i, \tilde{l}_i)$ iteratively until convergence is achieved.

C. Review of BT [6], [7]

In BT, the state-space realization (A, B, C) is first transformed into a balanced realization (A_b, B_b, C_b) using a similarity transformation T_b , such that:

$$A_b = T_b^{-1}AT, \quad B_b = T_b^{-1}B, \quad C_b = CT_b.$$

In a balanced realization, the controllability and observability Gramians are equal and diagonal. These Gramians satisfy the following equations:

$$A_b\Sigma + \Sigma A_b^T + B_bB_b^T = 0, \quad (14)$$

$$A_b^T\Sigma + \Sigma A_b + C_b^TC_b = 0, \quad (15)$$

where the diagonal elements of $\Sigma = \text{diag}(\sigma_1, \dots, \sigma_n)$ are the Hankel singular values of the system. These values are independent of the specific state-space realization and are ordered as $\sigma_i \geq \sigma_{i+1}$. Each σ_i represents the square root of the eigenvalue of the product of the controllability and observability Gramians, PQ , i.e., $\sigma_i = \sqrt{\lambda_i(PQ)}$.

In BT, the projection matrices are given by $V_r = T_b Z_r^T$ and $W_r = T_b^{-T} Z_r^T$, where $Z_r = [I_r \quad 0_{r \times (n-r)}]$. The truncated balanced realization is itself balanced, with equal and diagonal controllability and observability Gramians:

$$A_r\Sigma_r + \Sigma_r A_r^T + B_rB_r^T = 0, \quad (16)$$

$$A_r^T\Sigma_r + \Sigma_r A_r + C_r^TC_r = 0, \quad (17)$$

where

$$\Sigma = \begin{bmatrix} \Sigma_r & 0 \\ 0 & \Sigma_{n-r} \end{bmatrix}.$$

The truncated balanced realization retains the r largest Hankel singular values and approximates the full Gramians as $\Sigma \approx V_r\Sigma_rV_r^T$ and $\Sigma \approx W_r\Sigma_rW_r^T$.

III. MAIN WORK

Interpolation-based and Gramians-based MOR share the common feature of being projection techniques. In this section, we begin by highlighting that, while the projection matrices in both approaches satisfy Sylvester equations, there are significant differences in the specific Sylvester equations involved. Next, we explore the conditions under which the projection matrices nearly solve the same Sylvester equations, resulting in the construction of identical ROMs but with different state-space realizations. Using this framework, we demonstrate that BT and TSIA/IRKA can be viewed as approximations of each other under certain conditions.

Gramians-based MOR first rearranges the system's states based on a certain criterion via a similarity transformation T and then truncates the states considered less significant based on that criterion [4], [22]. Let the transformed realization be denoted as (A_t, B_t, C_t) , obtained through the similarity transformation T :

$$A_t = T^{-1}AT, \quad B_t = T^{-1}B, \quad C_t = CT.$$

The state-space equations for the transformed realization (A_t, B_t, C_t) are:

$$\begin{aligned} \dot{x}_t(t) &= A_t x_t(t) + B_t u(t), \\ y(t) &= C_t x_t(t). \end{aligned}$$

The controllability Gramian P_t and the observability Gramian Q_t for this realization are related to P and Q as follows:

$$P_t = T^{-1}PT^{-T}, \quad Q_t = T^TQT.$$

Let us partition T and T^{-T} as:

$$T = [V_r \quad T_1], \quad T^{-T} = [W_r \quad T_2].$$

Accordingly, the state-space realization (A_t, B_t, C_t) can be partitioned as:

$$A_t = \begin{bmatrix} A_r & A_{12} \\ A_{21} & A_{22} \end{bmatrix}, \quad B_t = \begin{bmatrix} B_r \\ B_2 \end{bmatrix}, \quad C_t = [C_r \quad C_2],$$

where $A_{12} = W_r^T A T_1$, $A_{21} = T_2^T A V_r$, $A_{22} = T_2^T A T_1$, $B_2 = T_2^T B$, and $C_2 = C T_1$. The corresponding partitioned state-space equations are:

$$\begin{aligned} \dot{x}_r(t) &= A_r x_r(t) + A_{12} \tilde{x}(t) + B_r u(t), \\ \dot{\tilde{x}}(t) &= A_{21} x_r(t) + A_{22} \tilde{x}(t) + B_2 u(t), \\ y(t) &= C_r x_r(t) + C_2 \tilde{x}(t). \end{aligned} \quad (18)$$

By neglecting the contribution of $\tilde{x}(t)$ to the system dynamics, the state-space equations (18) simplify to the ROM's state-space equations given in (3).

Note that P_t satisfies the following Lyapunov equation:

$$A_t P_t + P_t A_t^T + B_t B_t^T = 0. \quad (19)$$

Substituting $A_t = T^{-1}AT$ and $B_t = T^{-1}B$ into (19), and then pre-multiplying by T and post-multiplying by P_t^{-1} , we observe that T satisfies the following Sylvester equation:

$$\begin{aligned} T^{-1}ATP_t + P_t A_t^T + T^{-1}BB_t^T &= 0 \\ AT + TP_t A_t^T P_t^{-1} + BB_t^T P_t^{-1} &= 0 \\ AT - TS_{b,n} + BL_{b,n} &= 0, \end{aligned}$$

where

$$\begin{aligned} S_{b,n} &= -P_t A_t^T P_t^{-1} = \begin{bmatrix} S_{b,r} & S_{b,12} \\ S_{b,21} & S_{b,22} \end{bmatrix} \\ L_{b,n} &= B_t P_t^{-1} = \begin{bmatrix} L_{b,r} & L_{b,2} \end{bmatrix}. \end{aligned}$$

Next, partition P_t and P_t^{-1} as follows:

$$P_t = \begin{bmatrix} P_r & P_{12} \\ P_{12}^T & P_{22} \end{bmatrix}, \quad P_t^{-1} = \begin{bmatrix} P_{i,r} & P_{i,12} \\ P_{i,12}^T & P_{i,22} \end{bmatrix}.$$

From this, the following relations hold:

$$\begin{aligned} S_{b,r} &= -P_r A_r^T P_{i,r} - P_{12} A_{12}^T P_{i,r} \\ &\quad - P_r A_{21}^T P_{i,12} - P_{12} A_{22}^T P_{i,12}, \\ S_{b,12} &= -P_r A_r^T P_{i,12} - P_{12} A_{12}^T P_{i,12} \\ &\quad - P_r A_{21}^T P_{i,22} - P_{12} A_{22}^T P_{i,22}, \\ S_{b,21} &= -P_{12}^T A_r^T P_{i,r} - P_{22} A_{12}^T P_{i,r} \\ &\quad - P_{12}^T A_{21}^T P_{i,12} - P_{22} A_{22}^T P_{i,12}, \\ S_{b,22} &= -P_{12}^T A_r^T P_{i,12} - P_{22} A_{12}^T P_{i,12} \\ &\quad - P_{12}^T A_{21}^T P_{i,22} - P_{22} A_{22}^T P_{i,22}, \\ L_{b,r} &= B_r^T P_{i,r} + B_2^T P_{i,12}, \\ L_{b,2} &= B_2^T P_{i,22} + B_r^T P_{i,12}. \end{aligned}$$

It is also clear that V_r and T_1 satisfy the following Sylvester equations:

$$\begin{aligned} AV_r - V_r S_{b,r} + BL_{b,r} - T_1 S_{b,21} &= 0, \\ AT_1 - T_1 S_{b,22} + BL_{b,2} - V_r S_{b,12} &= 0. \end{aligned}$$

Similarly, Q_t is the solution of the following Lyapunov equation:

$$A_t^T Q_t + Q_t A_t + C_t^T C_t = 0. \quad (20)$$

Substituting $A_t = T^{-1}AT$ and $C_t = CT$ into (20), and pre-multiplying by T^{-T} and post-multiplying by Q_t^{-1} , we find that T^{-T} satisfies the following Sylvester equation:

$$\begin{aligned} A_t^T Q_t + Q_t A_t + C_t^T C_t &= 0 \\ T^T A^T T^{-T} Q_t + Q_t A_t + T^T C^T C_t &= 0 \\ A^T T^{-T} Q_t + T^{-T} Q_t A_t + C^T C_t &= 0 \\ A^T T^{-T} + T^{-T} Q_t A_t Q_t^{-1} + C^T C_t Q_t^{-1} &= 0 \\ A^T T^{-T} - T^{-T} S_{c,b} + C^T L_{c,n} &= 0, \end{aligned}$$

where

$$\begin{aligned} S_{c,n} &= -Q_t A_t Q_t^{-1} = \begin{bmatrix} S_{c,r} & S_{c,12} \\ S_{c,21} & S_{c,22} \end{bmatrix} \\ L_{c,n} &= C_t Q_t^{-1} = \begin{bmatrix} L_{c,r} & L_{c,2} \end{bmatrix}. \end{aligned}$$

Now, partition Q_t and Q_t^{-1} as

$$Q_t = \begin{bmatrix} Q_r & Q_{12} \\ Q_{12}^T & Q_{22} \end{bmatrix}, \quad Q_t^{-1} = \begin{bmatrix} Q_{i,r} & Q_{i,12} \\ Q_{i,12}^T & Q_{i,22} \end{bmatrix}.$$

From this, the following relations hold:

$$\begin{aligned} S_{c,r} &= -Q_r A_r Q_{i,r} - Q_{12} A_{21} Q_{i,r} \\ &\quad - Q_r A_{12} Q_{i,12}^T - Q_{12} A_{22} Q_{i,12}^T, \\ S_{c,12} &= -Q_r A_r Q_{i,12} - Q_{12} A_{21} Q_{i,12} \\ &\quad - Q_r A_{12} Q_{i,22} - Q_{12} A_{22} Q_{i,22}, \\ S_{c,21} &= -Q_{12}^T A_r Q_{i,r} - Q_{22} A_{21} Q_{i,r} \\ &\quad - Q_{12}^T A_{12} Q_{i,12}^T - Q_{22} A_{22} Q_{i,12}^T, \\ S_{c,22} &= -Q_{12}^T A_r Q_{i,12} - Q_{22} A_{21} Q_{i,12} \\ &\quad - Q_{12}^T A_{12} Q_{i,22} - Q_{22} A_{22} Q_{i,22}, \\ L_{c,r} &= C_r Q_{i,r} + C_2 Q_{i,12}^T, \\ L_{c,2} &= C_2 Q_{i,22} + C_r Q_{i,12}. \end{aligned}$$

Finally, it is evident that W_r and T_2 satisfy the following Sylvester equations:

$$\begin{aligned} A^T W_r - W_r S_{c,r} + C^T L_{c,r} - T_2 S_{c,21} &= 0, \\ A^T T_2 - T_2 S_{c,22} + C^T L_{c,2} - W_r S_{c,12} &= 0. \end{aligned}$$

A. Truncated Controllable Realization

We compute the eigenvalue decomposition of P as $P = T\Lambda_p T^T$, where $\Lambda_p = \text{diag}(\lambda_{p,1}, \dots, \lambda_{p,n})$ with $\lambda_{p,i} \geq \lambda_{p,i+1}$. The matrix T , when used as a similarity transformation, organizes the states in descending order of the eigenvalues of P ; for more details, see [7]. The weakly controllable states (the last $n - r$ states) can then be truncated. Since $T^{-T} = T$, we have $V_r = W_r$, implying that retaining the r most controllable states in the ROM constitutes a Galerkin projection problem. Moreover, in this case, P_t takes the form:

$$P_t = \begin{bmatrix} \Lambda_{p,r} & 0 \\ 0 & \Lambda_{p,n-r} \end{bmatrix},$$

where $\Lambda_{p,r} = \text{diag}(\lambda_{p,1}, \dots, \lambda_{p,r})$ and $\Lambda_{p,n-r} = \text{diag}(\lambda_{p,r+1}, \dots, \lambda_{p,n})$. Therefore, we have:

$$\begin{aligned} S_{b,r} &= -\Lambda_{p,r} A_r^T \Lambda_{p,r}^{-1}, & S_{b,21} &= -\Lambda_{p,n-r} A_{12}^T \Lambda_{p,r}^{-1}, \\ L_{b,r} &= B_r^T \Lambda_{p,r}^{-1}. \end{aligned}$$

When the truncated states are nearly uncontrollable, $\Lambda_{p,n-r} \approx 0$, leading to $S_{b,21} \approx 0$. As a result, the projection matrix V_r approximately solves the following Sylvester equation:

$$AV_r - V_r S_{b,r} + BL_{b,r} \approx 0.$$

Furthermore, we observe that $V_r \approx \hat{P}\Lambda_{p,r}^{-1}$. Consequently, $C\hat{P} - C_r\Lambda_{p,r} \approx 0$, which corresponds to the optimality condition (8) and the interpolation condition (11). In conclusion, when the truncated states are nearly uncontrollable,

the truncated controllable realization satisfies the interpolation condition (11). However, when the truncated states are more controllable, the approximation $P \approx V_r \Lambda_{p,r} V_r^T$ becomes less accurate, and the deviation of the truncated controllable realization from the interpolation condition (11) increases, depending on the controllability of the truncated states.

B. Truncated Observable Realization

We compute the eigenvalue decomposition of Q as $Q = T \Lambda_q T^T$, where $\Lambda_q = \text{diag}(\lambda_{q,1}, \dots, \lambda_{q,n})$ with $\lambda_{q,i} \geq \lambda_{q,i+1}$. The matrix T , when used as a similarity transformation, arranges the states in descending order of the eigenvalues of Q ; for more details, see [7]. The weakly observable states (the last $n-r$ states) can then be truncated. Since $T^{-T} = T$, we have $V_r = W_r$, implying that retaining the r most observable states in the ROM is a Galerkin projection problem. Furthermore, in this case, Q_t takes the form:

$$Q_t = \begin{bmatrix} \Lambda_{q,r} & 0 \\ 0 & \Lambda_{q,n-r} \end{bmatrix},$$

where $\Lambda_{q,r} = \text{diag}(\lambda_{q,1}, \dots, \lambda_{q,r})$ and $\Lambda_{q,n-r} = \text{diag}(\lambda_{q,r+1}, \dots, \lambda_{q,n})$. Therefore, we have:

$$\begin{aligned} S_{c,r} &= -\Lambda_{q,r} A_r \Lambda_{q,r}^{-1}, & S_{c,21} &= -\Lambda_{q,n-r} A_{21} \Lambda_{q,r}^{-1} \\ L_{c,r} &= C_r \Lambda_{q,r}^{-1}. \end{aligned}$$

When the truncated states are nearly unobservable, $\Lambda_{q,n-r} \approx 0$, leading to $S_{c,21} \approx 0$. As a result, the projection matrix W_r approximately solves the following Sylvester equation:

$$A^T W_r - W_r S_{c,r} + C^T L_{c,r} \approx 0.$$

Additionally, we observe that $W_r \approx \hat{Q} \Lambda_{q,r}^{-1}$. Consequently, $\hat{Q}^T B - \Lambda_{q,r} B_r \approx 0$, which corresponds to the optimality condition (9) and the interpolation condition (12). In conclusion, when the truncated states are nearly unobservable, the truncated observable realization satisfies the interpolation condition (12). However, when the truncated states are more observable, the approximation $Q \approx W_r \Lambda_{q,r} W_r^T$ becomes less accurate, and the deviation of the truncated observable realization from the interpolation condition (12) increases, depending on the observability of the truncated states.

C. Truncated Balanced Realization

In a truncated balanced realization, both the controllability Gramian and observability Gramian are equal and diagonal. This combines the two previously discussed cases, yielding:

$$P_t = Q_t = \Sigma = \begin{bmatrix} \Sigma_r & 0 \\ 0 & \Sigma_{n-r} \end{bmatrix}.$$

Thus, when the truncated states are nearly uncontrollable and unobservable, the corresponding Hankel singular values are close to zero, meaning $\Sigma_{n-r} \approx 0$. As a result, the projection matrices in BT approximately solve the following Sylvester equations:

$$\begin{aligned} A V_r + V_r \Sigma_r A_r^T \Sigma_r^{-1} + B B_r^T \Sigma_r^{-1} &\approx 0, \\ A^T W_r + W_r \Sigma_r A_r \Sigma_r^{-1} + C^T C_r \Sigma_r^{-1} &\approx 0. \end{aligned}$$

It follows that $V_r \approx \hat{P} \Sigma_r^{-1}$ and $W_r \approx \hat{Q} \Sigma_r^{-1}$. Consequently, we have $C \hat{P} - C_r \Sigma_r \approx 0$ and $\hat{Q}^T B - \Sigma_r B_r \approx 0$. Moreover, since $W_r^T V_r = I$, we also obtain $\hat{Q}^T \hat{P} - \Sigma_r^2 \approx 0$. This corresponds to the optimality conditions (8)–(10) and the corresponding interpolation conditions (11)–(13).

In conclusion, as long as the truncated states are nearly uncontrollable and unobservable, the truncated balanced realization nearly satisfies the interpolation conditions (11)–(13). However, when the truncated states have significant Hankel singular values, the approximations $P \approx V_r \Sigma_r V_r^T$ and $Q \approx W_r \Sigma_r W_r^T$ become less accurate, and the truncated balanced realization deviates from the interpolation conditions, with the deviation depending on the Hankel singular values of the truncated states.

The local optimum of $\|H(s) - H_r(s)\|_{\mathcal{H}_2}^2$ satisfies the following:

$$\begin{aligned} \|H(s) - H_r(s)\|_{\mathcal{H}_2}^2 &= \text{trace}(C P C_r^T - C_r P_r C_r^T) \\ &= \text{trace}(C(P - V_r P V_r^T) C^T) \\ &= \text{trace}(B^T Q B - B_r^T Q_r B_r) \\ &= \text{trace}(B^T (Q - W_r Q_r W_r^T) B). \end{aligned} \quad (21)$$

Thus, both TSIA and IRKA inherently focus on capturing the most controllable and observable states, ultimately capturing the Hankel singular values, as these values combine information about controllability and observability. When the order r of the reduced model is large enough to include all significant Hankel singular values, TSIA and IRKA are likely to capture them upon convergence. This is indicated by a small $\|H(s) - H_r(s)\|_{\mathcal{H}_2}$, implying that TSIA and IRKA have successfully captured the system's most controllable and observable states.

On the other hand, if the reduced model's order r is smaller than the number of significant Hankel singular values, TSIA and IRKA are less likely to capture all these values upon convergence, and achieving a small $\|H(s) - H_r(s)\|_{\mathcal{H}_2}$ becomes more difficult, as suggested by equation (21).

In summary, when the reduced model's order r is sufficient to capture all significant Hankel singular values, TSIA, IRKA, and BT are likely to produce the same ROM, though with different state-space realizations. If the model order is insufficient, TSIA and IRKA prioritize satisfying the \mathcal{H}_2 -optimality conditions, while BT focuses on retaining the largest Hankel singular values. In this case, BT deviates from the interpolation conditions (11)–(13), while TSIA and IRKA may not preserve the Hankel singular values. The degree of deviation depends on the magnitude of the truncated Hankel singular values. These observations are illustrated in Figure 1.

IV. NUMERICAL VALIDATION

In this section, we numerically validate the observations presented in this short note. We start with a small illustrative example and then move on to a high-order model to show that the findings of this research extend beyond simple toy examples. For \mathcal{H}_2 -optimal MOR, we have only considered IRKA for testing, as TSIA is equivalent to IRKA.

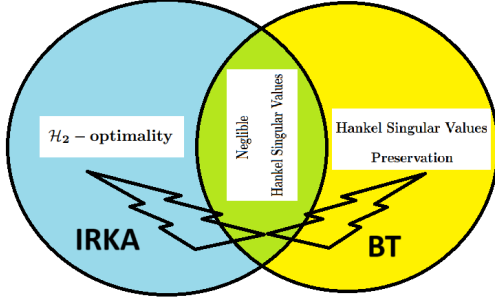


Fig. 1: BT and IRKA's divergence in behaviour as the order r is decreased

Illustrative Example: Consider the following 6th-order system:

$$A = \begin{bmatrix} -9 & -29 & -100 & -82 & -19 & -2 \\ 1 & 0 & 0 & 0 & 0 & 0 \\ 0 & 1 & 0 & 0 & 0 & 0 \\ 0 & 0 & 1 & 0 & 0 & 0 \\ 0 & 0 & 0 & 1 & 0 & 0 \\ 0 & 0 & 0 & 0 & 1 & 0 \end{bmatrix},$$

$$B = [1 \ 0 \ 0 \ 0 \ 0 \ 0]^T,$$

$$C = [0 \ 0 \ 0 \ 0 \ -1 \ 1].$$

The Hankel singular values of this system, rounded to four decimal places, are: 0.3725, 0.1361, 0.0137, 0.0013, 0.0011, 0.0000. Since the last singular value is zero at this precision, BT should generate a 5th-order local optimum for $\|H(s) - H_r(s)\|_{\mathcal{H}_2}^2$ without significant deviation from the optimality conditions (8)-(10). The 5th-order reduced model obtained by BT is:

$$A_r = \begin{bmatrix} -0.0340 & -0.1404 & -0.0609 & 0.0256 & 0.0029 \\ 0.1404 & -0.1597 & -0.2513 & 0.0905 & 0.0106 \\ -0.0609 & 0.2513 & -0.7975 & 0.7089 & 0.0683 \\ -0.0256 & 0.0905 & -0.7089 & -1.4171 & -3.3515 \\ 0.0029 & -0.0106 & 0.0683 & 3.3515 & -0.0207 \end{bmatrix}$$

$$B_r = [-0.1593 \ 0.2085 \ -0.1476 \ -0.0596 \ 0.0068]^T$$

$$C_r = [-0.1593 \ -0.2085 \ -0.1476 \ 0.0596 \ 0.0068].$$

One can verify that this state-space realization satisfies:

$$P_r = Q_r = \text{diag}(0.3725, 0.1361, 0.0137, 0.0013, 0.0011).$$

For this ROM, we obtain:

$$\|C\hat{P} - C_r P_r\|_2 = 1.5523 \times 10^{-10},$$

$$\|\hat{Q}^T B - Q_r B_r\|_2 = 1.5523 \times 10^{-10},$$

$$\|\hat{Q}^T \hat{P} - Q_r P_r\|_2 = 7.7531 \times 10^{-10}.$$

These results are consistent with the findings presented in this paper.

The penultimate Hankel singular value, 0.0011, is also close to zero. Consequently, we computed the 4th-order truncated balanced realization and obtained the following results:

$$\|C\hat{P} - C_r P_r\|_2 = 1.5478 \times 10^{-5},$$

$$\|\hat{Q}^T B - Q_r B_r\|_2 = 1.5478 \times 10^{-5},$$

$$\|\hat{Q}^T \hat{P} - Q_r P_r\|_2 = 6.5320 \times 10^{-6}.$$

These results confirm that the ROM effectively represents a local optimum. Next, we evaluated the deviations for the 1st-order truncated balanced realization, yielding:

$$\|C\hat{P} - C_r P_r\|_2 = 0.0033,$$

$$\|\hat{Q}^T B - Q_r B_r\|_2 = 0.0033,$$

$$\|\hat{Q}^T \hat{P} - Q_r P_r\|_2 = 0.0485.$$

Since the second Hankel singular value was somewhat significant, we observed noticeable deviations from Wilson's conditions [12].

Next, we generated a 5th-order initial guess using MATLAB's "rss" command, resulting in:

$$A_r^{(0)} = \begin{bmatrix} -2.6934 & 2.6255 & 2.1559 & 3.6127 & -0.3077 \\ -3.9154 & 2.3707 & -2.2304 & 5.9836 & -1.5464 \\ 1.5037 & 1.2914 & -2.3212 & 2.0516 & -0.0588 \\ 0.4274 & -3.1587 & -0.6928 & -7.7081 & 0.6261 \\ -1.5911 & -2.5749 & -1.5223 & -3.2990 & -3.9306 \end{bmatrix},$$

$$B_r^{(0)} = [-0.0301 \ -0.1649 \ 0.6277 \ 0 \ 1.1093]^T,$$

$$C_r^{(0)} = [-0.8637 \ 0.0774 \ 0 \ 0 \ -0.0068].$$

The Hankel singular values of this initial guess are: 0.1703, 0.1169, 0.0174, 0.0000, 0.0000. These values are significantly different from those of the original system. We then used IRKA, starting with the mirror images of the poles and their associated residuals from this initial guess. After convergence, we obtained the following ROM:

$$A_r = \begin{bmatrix} -2.6352 & 0.0671 & -0.9963 & 0.5576 & 0.4301 \\ -50.1054 & 0.1552 & -12.0011 & 15.5128 & 16.1474 \\ 4.1681 & -0.3263 & 1.1660 & -0.4096 & -0.2116 \\ 4.8020 & -0.4227 & 0.7610 & -0.3709 & -0.2280 \\ 7.0043 & -0.6133 & 2.7409 & -1.2318 & -0.7451 \end{bmatrix},$$

$$B_r = [-0.0259 \ -0.4306 \ 0.0255 \ 0.0376 \ 0.0561]^T,$$

$$C_r = [-0.2488 \ 0.0035 \ 1.0315 \ 0.4051 \ -0.8252].$$

This reduced model satisfies:

$$\|C\hat{P} - C_r P_r\|_2 = 1.3865 \times 10^{-15},$$

$$\|\hat{Q}^T B - Q_r B_r\|_2 = 6.5922 \times 10^{-14},$$

$$\|\hat{Q}^T \hat{P} - Q_r P_r\|_2 = 7.1162 \times 10^{-12}.$$

These results confirm that the model is an \mathcal{H}_2 local optimum. We then transformed this reduced-order realization into its balanced form via similarity transformation. The balanced realization obtained is:

$$A_r = \begin{bmatrix} -0.0340 & -0.1404 & 0.0609 & 0.0256 & -0.0029 \\ 0.1404 & -0.1597 & 0.2513 & 0.0905 & -0.0106 \\ 0.0609 & -0.2513 & -0.7975 & -0.7090 & 0.0683 \\ -0.0256 & 0.0905 & 0.7090 & -1.4181 & 3.3518 \\ -0.0029 & 0.0106 & 0.0683 & -3.3518 & -0.0207 \end{bmatrix},$$

$$B_r = [-0.1593 \ 0.2085 \ 0.1476 \ -0.0596 \ -0.0068]^T,$$

$$C_r = [-0.1593 \ -0.2085 \ 0.1476 \ 0.0596 \ -0.0068].$$

This transformed ROM is identical to the one obtained using BT.

Next, we generated a 1st-order initial guess using MATLAB's "rss" command:

$$A_r^{(0)} = -0.4211, \quad B_r^{(0)} = -0.1649, \quad C_r^{(0)} = 0.6277.$$

The Hankel singular value for this initial guess is 0.1229, which does not match the Hankel singular values of $H(s)$. We then initiated IRKA with the mirror images of the poles

and their associated residuals from this initial guess. After convergence, the resulting ROM is:

$$A_r = -0.0507, \quad B_r = -0.0319, \quad C_r = -0.9482.$$

This model satisfies:

$$\begin{aligned} \|CP_{12} - C_r P_r\|_2 &= 3.6500 \times 10^{-9}, \\ \|Q_{12}^T B - Q_r B_r\|_2 &= 1.0866 \times 10^{-7}, \\ \|Q_{12}^T P_{12} - Q_r P_r\|_2 &= 7.1412 \times 10^{-5}. \end{aligned}$$

This confirms that the ROM is indeed a local optimum for $\|H(s) - H_r(s)\|_{\mathcal{H}_2}^2$. The Hankel singular value of this ROM is 0.2978, showing that IRKA prioritized satisfying the optimality conditions and approximated 0.3725 with 0.2978. This verifies the observations summarized in Figure 1.

International Space Station: Consider the 270th-order international space station model from [23], which has 3 inputs and 3 outputs. Figure 2 displays the Hankel singular values for 40th-order reduced models generated by both BT and IRKA. It is evident that both algorithms preserve the most significant 40 Hankel singular values of $H(s)$. Furthermore, the ROM

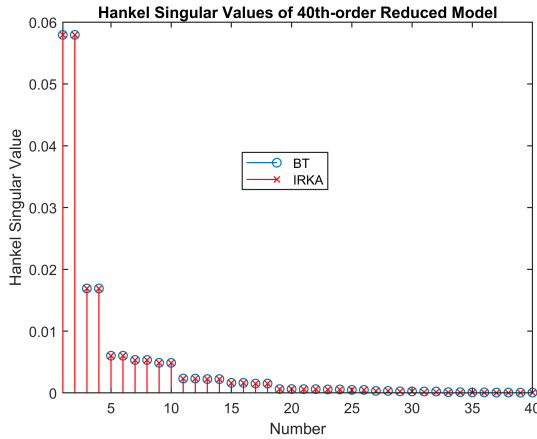


Fig. 2: Hankel singular values comparison

obtained from BT satisfies:

$$\begin{aligned} \|C\hat{P} - C_r P_r\|_2 &= 9.5788 \times 10^{-8}, \\ \|\hat{Q}^T B - Q_r B_r\|_2 &= 9.8014 \times 10^{-8}, \\ \|\hat{Q}^T \hat{P} - Q_r P_r\|_2 &= 8.7005 \times 10^{-9}. \end{aligned}$$

This confirms that it is a local optimum for $\|H(s) - H_r(s)\|_{\mathcal{H}_2}^2$.

Next, Figure 3 presents the Hankel singular values for 5th-order reduced models generated by BT and IRKA. IRKA accurately captured 4 of the Hankel singular values but missed the 5th. The ROM produced by BT yields the following results:

$$\begin{aligned} \|C\hat{P} - C_r P_r\|_2 &= 3.0169 \times 10^{-7}, \\ \|\hat{Q}^T B - Q_r B_r\|_2 &= 3.0012 \times 10^{-7}, \\ \|\hat{Q}^T \hat{P} - Q_r P_r\|_2 &= 3.6124 \times 10^{-5}. \end{aligned}$$

Interestingly, while IRKA successfully captures the first 4 Hankel singular values of $H(s)$, BT effectively achieves a local optimum for $\|H(s) - H_r(s)\|_{\mathcal{H}_2}^2$.

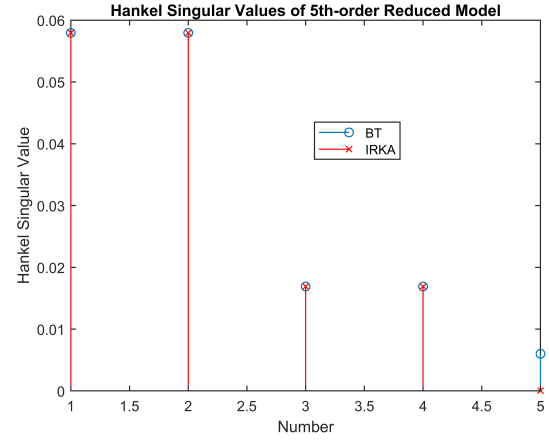


Fig. 3: Hankel singular values comparison

V. CONCLUSION

This brief establishes a connection between Gramians-based MOR and interpolation-based \mathcal{H}_2 -optimal reduction. It demonstrates that retaining the most controllable or observable states in the ROM corresponds to satisfying a subset of the \mathcal{H}_2 -optimality conditions, provided the truncated states are weakly controllable or observable. Additionally, it shows that preserving the states with dominant Hankel singular values ensures all \mathcal{H}_2 -optimality conditions are met, as long as the truncated states are associated with negligible Hankel singular values. Furthermore, the results reveal that meeting the \mathcal{H}_2 -optimality conditions in algorithms like IRKA or TSIA inherently preserves the Hankel singular values. Therefore, BT can be viewed as an approximate \mathcal{H}_2 -optimal MOR algorithm, and IRKA/TSIA can be seen as approximations of BT, yielding almost identical ROMs but with different state-space realizations, as long as the reduced model's order is large enough to capture all significant Hankel singular values. Numerical examples are provided to validate these claims. The results of this paper not only establish a strong connection between BT and IRKA/TSIA but also pave the way for achieving approximate truncated balanced realizations through interpolation, eliminating the need to solve high-order Lyapunov equations.

REFERENCES

- [1] A. Quarteroni, G. Rozza *et al.*, *Reduced order methods for modeling and computational reduction*. Springer, 2014, vol. 9.
- [2] P. Benner, V. Mehrmann, and D. C. Sorensen, *Dimension reduction of large-scale systems*. Springer, 2005, vol. 45.
- [3] G. Obinata and B. D. Anderson, *Model reduction for control system design*. Springer Science & Business Media, 2012.
- [4] A. C. Antoulas, *Approximation of large-scale dynamical systems*. SIAM, 2005.
- [5] W. H. Schilders, H. A. Van der Vorst, and J. Rommes, *Model order reduction: theory, research aspects and applications*. Springer, 2008, vol. 13.
- [6] B. Moore, "Principal component analysis in linear systems: Controllability, observability, and model reduction," *IEEE Transactions on Automatic Control*, vol. 26, no. 1, pp. 17–32, 1981.
- [7] D. F. Enns, "Model reduction with balanced realizations: An error bound and a frequency weighted generalization," in *The 23rd IEEE Conference on Decision and Control*. IEEE, 1984, pp. 127–132.

- [8] S. Gugercin and A. C. Antoulas, "A survey of model reduction by balanced truncation and some new results," *International Journal of Control*, vol. 77, no. 8, pp. 748–766, 2004.
- [9] V. Balakrishnan, Q. Su, and C.-K. Koh, "Efficient balance-and-truncate model reduction for large scale systems," in *Proceedings of the 2001 American Control Conference.(Cat. No. 01CH37148)*, vol. 6. IEEE, 2001, pp. 4746–4751.
- [10] S. Gugercin, A. C. Antoulas, and C. Beattie, " \mathcal{H}_2 model reduction for large-scale linear dynamical systems," *SIAM Journal on Matrix Analysis and Applications*, vol. 30, no. 2, pp. 609–638, 2008.
- [11] P. Van Dooren, K. A. Gallivan, and P.-A. Absil, " \mathcal{H}_2 -optimal model reduction of MIMO systems," *Applied Mathematics Letters*, vol. 21, no. 12, pp. 1267–1273, 2008.
- [12] D. Wilson, "Optimum solution of model-reduction problem," in *Proceedings of the Institution of Electrical Engineers*, vol. 117, no. 6. IET, 1970, pp. 1161–1165.
- [13] Y. Xu and T. Zeng, "Optimal \mathcal{H}_2 model reduction for large scale MIMO systems via tangential interpolation," *International Journal of Numerical Analysis & Modeling*, vol. 8, no. 1, 2011.
- [14] P. Benner, M. Köhler, and J. Saak, "Sparse-dense Sylvester equations in \mathcal{H}_2 -model order reduction," Max Planck Institute Magdeburg, Preprint MPIMD/11-11, Dec. 2011, available from <http://www.mpi-magdeburg.mpg.de/preprints/>.
- [15] A. C. Antoulas, C. A. Beattie, and S. Gugercin, *Interpolatory methods for model reduction*. SIAM, 2020.
- [16] A. Astolfi, G. Scarciotti, J. Simard, N. Faedo, and J. V. Ringwood, "Model reduction by moment matching: Beyond linearity a review of the last 10 years," in *2020 59th IEEE Conference on Decision and Control (CDC)*. IEEE, 2020, pp. 1–16.
- [17] A. Astolfi, "Model reduction by moment matching for linear and nonlinear systems," *IEEE Transactions on Automatic Control*, vol. 55, no. 10, pp. 2321–2336, 2010.
- [18] T. C. Ionescu, J. M. Scherpen, O. V. Iftime, and A. Astolfi, "Balancing as a moment matching problem," in *Proc. 20th Int. Symp. on Mathematical Theory of Networks and Sys*, 2012.
- [19] Y. Kawano, T. C. Ionescu, and O. V. Iftime, "Gramian preserving moment matching for linear systems," in *2023 European Control Conference (ECC)*. IEEE, 2023, pp. 1–6.
- [20] K. Gallivan, A. Vandendorpe, and P. Van Dooren, "Sylvester equations and projection-based model reduction," *Journal of Computational and Applied Mathematics*, vol. 162, no. 1, pp. 213–229, 2004.
- [21] T. Wolf, " \mathcal{H}_2 pseudo-optimal model order reduction," Ph.D. dissertation, Technische Universität München, 2014.
- [22] D. C. Sorensen and A. Antoulas, "The Sylvester equation and approximate balanced reduction," *Linear Algebra and Its Applications*, vol. 351, pp. 671–700, 2002.
- [23] Y. Chahlaoui and P. Van Dooren, "Benchmark examples for model reduction of linear time-invariant dynamical systems," in *Dimension Reduction of Large-Scale Systems: Proceedings of a Workshop held in Oberwolfach, Germany, October 19–25, 2003*. Springer, 2005, pp. 379–392.